Mon. Not. R. Astron. Soc. **000**, 1–14 (2002) Printed 23 June 2011 (MN LATEX style file v2.2)

Photometric redshifts and K-corrections for the Sloan Digital Sky Survey Data Release 7

Ana Laura O'Mill,[1,2⋆] Fernanda Duplancic,[1,2] Diego García Lambas,[1,2] & Laerte Sodré Jr[3]
[1] *Instituto de Astronomía Teórica y Experimental, IATE, Observatorio Astronómico, Universidad Nacional de Córdoba, Laprida 854, X5000BGR, Córdoba Argentina*
[2] *Consejo de Investigaciones Científicas y Técnicas (CONICET), Avenida Rivadavia 1917, C1033AAJ, Buenos Aires, Argentina*
[3] *Departamento de Astronomia, Instituto de Astronomia, Geofísica e Ciências Atmosféricas da USP, Rua do Matão 1226, Cidade Universitária, 05508-090, São Paulo, Brazil*

Released 2010 Xxxxx XX

ABSTRACT
We present a catalogue of galaxy photometric redshifts and k-corrections for the Sloan Digital Sky Survey Seven Data Release (SDSS-DR7), available on the World Wide Web. The photometric redshifts were estimated with an artificial neural network using five *ugriz* bands, concentration indices and Petrosian radii in the g and r bands. We have explored our redshift estimates with different training set concluding that the best choice to improve redshift accuracy comprises the Main Galaxies Sample (MGS), the Luminous Red Galaxies, and galaxies of active galactic nuclei covering the redshift range $0 < z \leqslant 0.3$. For the MGS, the photometric redshift estimates agree with the spectroscopic values within $rms = 0.0227$. The derived distribution of photometric redshifts in the range $0 < z_{\rm phot} \leqslant 0.6$ agrees well with the model predictions.
k-corrections were derived by calibration of the `k-correct_v4.2` code results for the MGS with the reference frame ($z = 0.1$) $(g - r)$ colours. We adopt a linear dependence of k corrections on redshift and $(g - r)$ colours that provide suitable distributions of luminosity and colours for galaxies up to redshift $z_{\rm phot} = 0.6$ comparable to the results in the literature. Thus, our k-correction estimate procedure is a powerful, low computational time algorithm capable of reproducing suitable results that can be used for testing galaxy properties at intermediate redshifts using the large SDSS database.

Key words: galaxies: distances and redshifts - galaxies: formation - cosmology: theory

1 INTRODUCTION

The knowledge of distances to galaxies is important to deduce intrinsic galaxy properties (absolute magnitude, size, etc.) from the observed properties (colours, sizes, angles, flux, apparent size, etc.).
Since pioneering works measuring redshift of bright galaxies (e.g., (Shapley (1932), Humason et al. (1956)), many efforts have been invested in mapping the light and matter in the Universe. Statistical analysis of galaxy properties and systems can be invaluable tools to study large-scale structure and evolution in the universe.
In recent years, multi-band photometry has been performed for several millions of galaxies, whereas spectroscopic redshifts have been measured only for a small fraction of the photometric data. The Sloan Digital Sky survey has obtained multi-band images for approximately one hundred billion galaxies (and the next surveys foresee increasing the number of objects up to billions), while spectroscopic measurements have been obtained for nearly one million galaxies. A solution to the difficulty of obtaining spectroscopic redshifts relies on the use of photometric redshift techniques. Although the redshifts calculated through these techniques are far less accurate than the spectroscopic measurements, these approximate distance estimates allow for useful analysis in fields such as extragalactic astronomy and observational cosmology.

Two basic family of methods are commonly employed to calculate photometric redshifts. In the template matching approach, a set of spectral energy distribution (SED) templates is fitted to the observations (e.g., colours). In the empirical approach, on the other side, photometric redshifts are obtained from a large and representative training set of galaxies with both photometry and precise redshift estimations. The advantage of the first method is that it can also provide additional information, like the spectral type, k-corrections and absolute magnitudes. The accuracy of these estimations is limited by the SED models. The empirical model overcomes this limitation through the use of a training set which,

⋆ E-mail: aomill@oac.uncor.edu

however, should be large and representative enough to provide accurate redshift estimations.

The observed spectral energy distribution of distant galaxies is redshifted with respect to that in the galaxy rest frame. The k-correction term (Oke & Sandage 1968; Hogg et al. 2001) applied to the apparent magnitude measured in a given photometric band takes into account this effect, allowing to compare photometric properties of galaxies at different redshifts. The estimation of k-corrections, then, is a requirement for many studies of distant galaxies. It is possible to model k-corrections as a function of redshift and galaxy morphological type (Fukugita et al. 1995; Mannucci et al. 2001). Lahav et al. (1995) and Banerji et al. (2010) use ANNs to obtain morphological classification of galaxies. However, these techniques employ as training sets, objects that had been classified by human eye subject to some degree of ambiguity and uncertainty, particularly at large redshifts.

A more direct way to obtain k-corrections is by modelling galaxy SEDs as a function of wavelength. Usually template fitting of observed galaxy fluxes is employed to reconstruct the SED of the galaxy (Blanton et al. (2003), Blanton & Roweis (2007)). The feasibility and accuracy of this method relies in the quality of the models.

For objects with spectral data, k-corrections can also be obtained directly. Roche et al. (2009) used this technique to calculate k-corrections for early-type galaxies from the SDSS-DR6, providing individual estimates for each galaxy. However, this technique is restricted to a limited number of galaxies with spectroscopy.

Recent works (Chilingarian et al. (2010), Westra et al. (2010)) have approximated k-corrections with analytical functions of redshift, parametrized with some property characterizing galaxy type. Chilingarian et al. (2010) used different observed colour indices to approximate k-corrections for nine filters ($ugrizYJHK$). Westra et al. (2010) used spectra from the Smithsonian Hectospec Lensing Survey to obtain direct measurements of k-corrections by parametrization with the ratio of the average flux red and bluewards of the 4000Å break (D_n4000). These kinds of parametrization simplify the computation of k-corrections and improve their accuracy.

In this paper, we present a galaxy photometric redshift ($z_{\rm phot}$) catalogue and a method for calculating k-corrections, for the seventh Data Release (DR7) of the Sloan Digital Sky Survey (SDSS) imaging catalogue (Blanton et al. (2003), Eisenstein et al. (2001), Gunn et al. (1998), Strauss et al. (2002), York et al. (2000)). To compute photometric redshifts we used the ANNz software package (Collister & Lahav (2004)), which have been shown to be a reliable tool. There are also two sets of photometric redshifts in the SDSS database: Abazajian et al. (2009) employ empirical, template-based and hybrid-techniques approaches to photometric redshift estimation, whereas Oyaizu et al. (2008) adopt a neural network method and provide two different estimations, D1 and CC2. Here we also compare our redshift estimations with those in the CC2 catalogue from Oyaizu et al. (2008), which uses colours and concentration indices to infer redshifts. For the computation of k-corrections we propose a joint parametrization in terms of redshift and the $(g-r)$ colour in a certain reference frame for all SDSS bands, as well as an algorithm to determine them from the photometric data. We compare our results with those found in literature.

This paper is organized as follows. In Section 2 we describe the data used in our analysis. Section 3 presents our approach to calculate photometric redshifts in SDSS-DR7, analysing their advantages and limitations. Our estimation of k-corrections is presented in Section 4. Finally, Section 5 summarizes the results obtained in this work.

Throughout this paper, we adopt a cosmological model characterized by the parameters $\Omega_m = 0.3$, $\Omega_\Lambda = 0.7$ and $H_0 = 75\,h\,{\rm km\,s^{-1}\,Mpc^{-1}}$.

2 THE GALAXY SAMPLES

The samples of galaxies used in this work were drawn from the Sloan Digital Sky Survey Seven Data Release (SDSS-DR7, Abazajian et al. (2009)). SDSS (York et al. (2000)) mapped more than one-quarter of the entire sky, performing photometry and spectroscopy for galaxies, quasars and stars. SDSS-DR7 is the seventh major data release, corresponding to the completion of the survey SDSS-II. It comprises 11.663 sq. deg. of imaging data, with an increment of ~ 2000 sq. deg., over the previous data release, lying in regions of low Galactic latitude. SDSS-DR7 provides imaging data for 357 million distinct objects in five bands, *ugriz*, as well as spectroscopy over $\simeq \pi$ steradians in the North Galactic cap and 250 square degrees in the South Galactic cap. The average wavelengths corresponding to the five broad bands are 3551, 4686, 6165, 7481, and 8931 Å (Fukugita et al. 1996; Hogg et al. 2001; Smith et al. 2002). For details regarding the SDSS camera see Gunn et al. (1998); for astrometric calibrations see Pier et al. (2003). The survey has completed spectroscopy over 9380 sq. deg.; the spectroscopy is now complete over a large contiguous area of the Northern Galactic Cap, closing the gap that was present in previous data releases.

In this work we have extracted two galaxy data sets from SDSS-DR7, one with spectroscopic redshifts measurements and the other consisting in photometric data.

The spectroscopic data was derived from the `fits` files at the SDSS home page[1]. consisting in Main Galaxy Sample (MGS; Strauss et al. (2002)), the Luminous Red Galaxy sample (LRG; Eisenstein et al. (2001)) and active galactic nuclei (AGN; Kauffmann et al. (2003)). These spectroscopic samples were used for the computation of photometric redshifts and calibration of k-corrections.

We built a first sample (hereafter Sz1) consisting in 80% of the objects from MGS, 10% from LRG and 10% from AGNs, combined into a single set comprising ~ 550000 galaxies. This sample was divided at random into two subsamples with the same number of objects generating a training and a validation set in order to calibrate the ANNz code used to the estimation of photometric redshifts.

As a testing set for the photometric redshifts we used a random sample (hereafter Sz2) of 60,000 objects from MGS. We excluded from this sample galaxies belonging to the training set to avoid undesirable biases.

For the calibration of k-corrections we used the full MGS. Following Montero-Dorta & Prada (2009), we have taken the magnitude range where the number of galaxies per solid angle rises at a constant rate as a function of redshift in each SDSS band. Therefore, the apparent magnitude limits are set to ensure that the effect of incompleteness is small in our sample. The adopted apparent magnitude limits in each band are : $u < 19.0$, $g < 17.91$,

[1] http://www.sdss.org/dr7/products/spectra/getspectra.html

Table 1. Description of the samples used in this work.

sample name	number of objects	Description
Sz1	~ 550000	Selected from SDSS-DR7 spectroscopic data. Used as training and validation sets in the computation of photometric redshifts
Sz2	~ 70000	Selected from SDSS-DR7 MGS (excluding training set galaxies). Used as testing set for photometric redshifts.
Sz3	~ 82000	Selected from SDSS-DR6 photometric data. Used to compare photometric redshift estimation with Oyaizu et al. (2008).
Sk1	~ 122000	Selected from SDSS-DR7 MGS taking into account apparent magnitude and redshift limits (see text). Used for k-correction calibration.
Sk2	~ 575000	Selected from SDSS-DR7 photometric data with our photometric redshifts estimation. Used to compute k-correction at higher redshift and compare with literature.

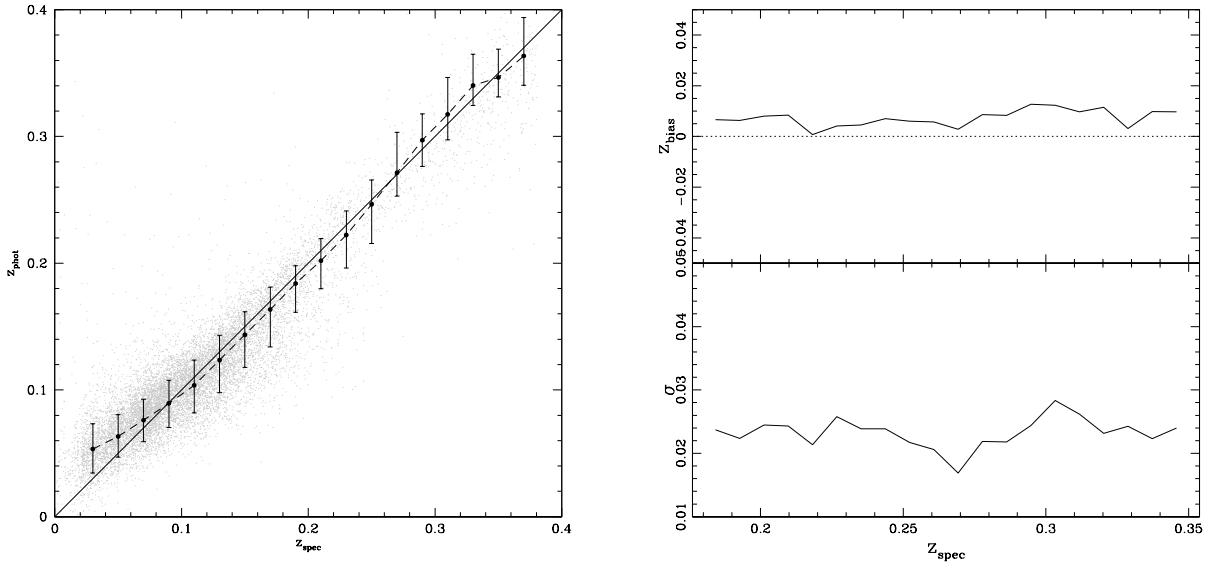

Figure 1. Left panel: $z_{\rm spec}$ vs $z_{\rm phot}$ relation for Sz2 sample (grey dots). The dashed line corresponds to the median value of the photometric redshift estimated at a given spectroscopic redshift interval. Error bars correspond to the 10 and 90 percentiles associated to the median. The solid line shows the one-to-one relation. Right panels: systematic (top right) and stochastic (bottom right) errors in the photometric redshift estimates.

$r < 17.77$, $i < 17.24$, and $z < 16.97$. For these limits we consider galaxies with $z_{spec} < 0.15$ to assure completeness in the u and g bands, and $z_{spec} < 0.18$ in the r, i and z bands. With these magnitude and redshift constraints, the sample used to calibrate the k-corrections (hereafter Sk1) contains ~ 122000 galaxies.

The photometric data set were extracted from the `Galaxy` table of the `CasJobs`[2] database. We restrict our analysis to photometric objects with $r < 21.5$, since this magnitude limit assures good photometric quality and a reliable star-galaxy separation (Stoughton et al., 2002, Scranton et al., 2002).

In order to contrast our estimates with those obtained by similar methods, we compare our results with photometric redshifts from Oyaizu et al. (2008). Taking into account these authors recommendation we use `PhotozCC2` estimates (obtained from colours and concentration indices, see Oyaizu et al. (2008)). It should be noted that `Photoz2` table was not updated for SDSS-DR7, so we have constructed a sample from SDSS-DR6 photometric data selecting at random 82000 objects with `PhotozCC2` redshift information [3]. For this sample we calculated photometric redshifts through the methods described in this work. Hereafter we will call this sample as Sz3.

In order to compute k-correction at higher redshifts we have selected a random sample of ~ 575000 photometric SDSS-DR7 data for which we have determined photometric redshifts and k-corrections (sample Sk2). For this sample we have also compared the k-corrections computed in this work with different results obtained from the literature.

[2] http://cas.sdss.org/dr7/

[3] SDSS-DR6 photometric data was downloaded from CasJobs just as DR7 photometric data including redshift information from Photoz2 table

Table 1 summarizes the main characteristics of the different samples used in this work

3 PHOTOMETRIC REDSHIFTS

Photometric redshift techniques use photometric parameters to perform an estimation of galaxy redshift. This technique can be used to infer efficiently large numbers of galaxy distances, even for faint galaxies, for which spectroscopic measurements are prohibitive because they would require large amounts of telescope time.

There are different techniques to estimate photometric redshifts which can be classified into two groups. The first set of techniques makes use of a small number of model galaxy spectra derived from empirical or model-based spectral energy distributions (SEDs). These methods estimate a galaxy redshift by finding an optimal combination of template spectra that reconstructs the observed galaxy colours (e.g., Benitez 2000; Bolzonella et al. 2000; Csabai et al. 2003). The fact that these methods rely on a small number of template SEDs is their main disadvantage, in particular for galaxies at high redshifts, since a representative set of spectral templates applicable at all redshifts is not easy to obtain. The second group, called empirical methods (e.g., Connolly et al. 1995; Brunner et al. 1999), comprises techniques that need a large amount of prior redshift information, in general in the form of training set. This class of methods aims to derive a parametrization for the redshift as a function of photometric parameters. The form of this parametrization is obtained through the use of a suitably large and representative training set of galaxies for which we have both photometry and precisely known redshifts. In this case we can use combinations of galaxy photometric parameters, such as magnitudes in different photometric bands, galaxy colours, and concentration indices. The main drawback of empirical methods is that the training set should be representative of the sample of galaxies for which we want to estimate photometric redshifts.

3.1 Method

We used Sz1 sample to compute photometric redshifts with the ANNz software package (Collister & Lahav (2004)), which uses an Artificial Neural Network (ANN) to parametrize the relation between redshift and photometric parameters. ANNz is based on a "multilayer perceptron"(MLP) algorithm, where the nodes are disposed in layers, and the nodes in a given layer are connected to all the nodes in adjacent layers. The ANN topology adopted in ANNz can be described as N_{in}:N_1:N_2:...:N_{out}, where N_{in} and N_{out} are, respectively, the number of input and output parameters, whereas N_i is the number of nodes in the $i-$th intermediate layer (e.g., Bishop 1991). The first layer contains the inputs, which in our application are photometric parameters. The final layer contains the outputs, in this case the photometric redshift ($z_{\rm phot}$).

The free parameters of ANNz are the "weights" between the nodes, and are obtained by "training" the ANN with a training set consisting of galaxies with spectroscopic redshifts. The selected training set must be large enough and representative of the target population, to assure a reliable mapping of the input into the output. Also, it must contain the same set of input parameters than the target sample, for which we want to estimate the photometric redshifts.

ANNz can be trained with different sets of input parameters in order to improve the photometric redshift accuracy. We have analysed several sets: i) magnitudes in the five SDSS bands, ii) colours and concentration index, iii) colours and Petrosian radii, and iv) SDSS-DR7 magnitudes in the five bands, plus concentration indices and Petrosian radii in g and r-bands. We found that the latter set is the best choice for redshift estimation. The use of concentration indices helps to break the degeneracies in the redshift-colour relation. This occurs due to the good correlation between the colour of a galaxy with its concentration indices and Petrosian radii. The resulting ANNz architecture adopted here is $9:14:14:14:1$.

3.2 Results

Our results of the ANNz training are shown in Figure 1. The left panel of Figure 1 shows the spectroscopic ($z_{\rm spec}$) vs. photometric ($z_{\rm phot}$) redshift relation for the testing sample Sz2. As explained in Section 2, galaxies in the training set were excluded from the sample in order to avoid bias in this comparison. This figure also shows the one-to-one relation as a solid line, the median value of the photometric redshift estimated at a given spectroscopic redshift interval (dashed line) and 10 and 90 percentiles (as error bars) of the scatter plot. The small dispersion seen in this figure corresponds to $rms \sim 0.0227$. For the MGS of the SDSS-EDR Collister & Lahav (2004) obtained $rms \sim 0.0229$ and for a sample comprising galaxies from SDSS-MGS, SDSS-LRG, CNOC2, CFRS, DEEP2 DEEP2, TKRS and 2SLAQ surveys, Oyaizu et al. (2008) obtained $rms \sim 0.03$. The right panel of Figure 1 shows the systematic differences between $z_{\rm phot}$ and $z_{\rm spec}$, z_{bias} (higher sub-panel), and the rms dispersion σ (lower sub-panel) as a function of redshift. Both, the bias and dispersion, shown little dependence with the spectroscopic redshift.

For comparison with other estimates, for LRGs, Abdalla et al. (2008) and Collister et al. (2007) used the ANNZ code to compute a refined star/galaxy probability based on a range of photometric parameters. The photometric redshift rms deviation is 0.049 when averaged for all galaxies, and 0.040 for a bright sub-sample with $i < 19.0$ in the redshift range $z_{\rm phot} = 0.4$ to 0.7.

In Figure 2 (top panel) we show the distribution of photometric redshifts $N(z)$ for Sz3 sample. In short dashed lines we display $N(z)$ for our calculation, and in dotted lines Oyaizu et al. (2008) estimates. The solid curve corresponds to the expected distribution given by the theoretical calculation of Blanton et al. (2003), assuming an universal luminosity function with parameters extracted from SDSS data. For $z_{\rm phot} < 0.1$ the observed distributions are similar to the expected prediction. For photometric redshifts between $z_{\rm phot} \sim 0.1$ and $z_{\rm phot} \sim 0.35$ our estimates are in better agreement with the theoretical curve, while Oyaizu et al. (2008) results show a $\sim 20\%$ deficit. We note that this range is very important because SDSS-DR7 data has reliable completeness up to $z_{\rm phot} < 0.35$, since beyond this redshift the galaxy density drops significantly. For $z_{\rm phot} \sim 0.4$ the observed distributions tend to overestimate the theoretical curve, an effect that could be associated to the Balmer break shifting between the g and r filters, difficulting the redshift estimates (Budavári et al. (2001)). The bottom panel of Figure 2 show the comparison between Oyaizu et al. (2008) $z_{\rm phot}$ and our estimates.

In Figure 2 (bottom panel) shows the $z_{\rm phot}$ redshift relation for Oyaizu et al. (2008) estimates and our estimates.

In O'Mill et al. (2008) it is estimated the maximum redshift (z_{max}) beyond which compact galaxies are confused with the im-

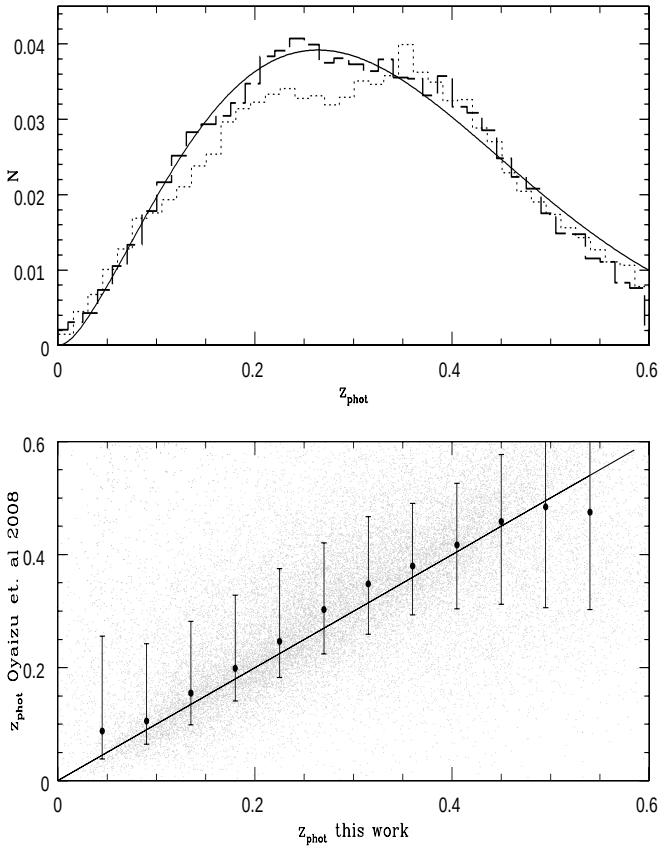

Figure 2. Top panel: distribution of photometric redshifts N(z) for our calculation (short dashed) and Oyaizu et al. 2008 (dotted) estimates. The solid curve corresponds to the expected distribution given by the theoretical calculation of Blanton et al. 2003. Bottom panel: the $z_{\rm phot}$ redshift relation for Oyaizu et al. (2008) estimates and our estimates. The dashed line corresponds to the median value and error bars correspond to the 10 and 90 percentiles associated to the median.

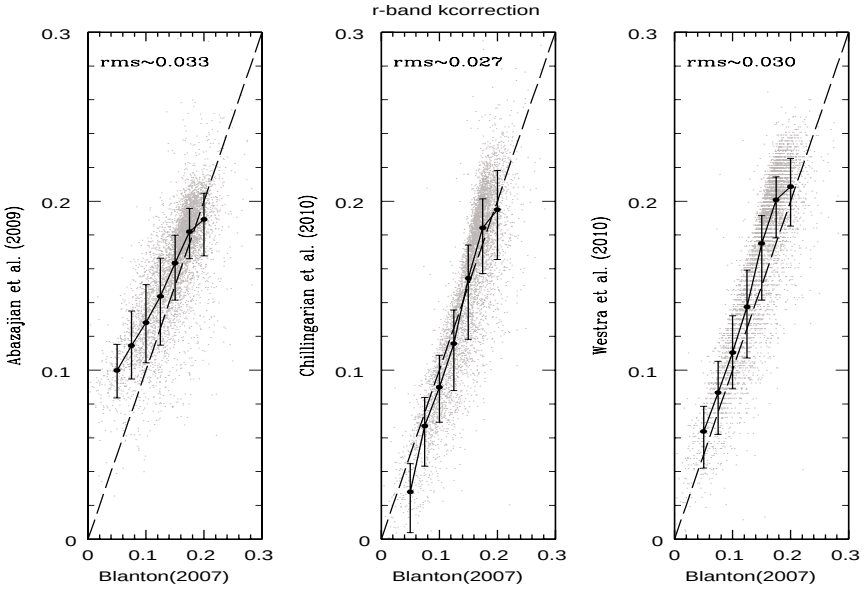

Figure 3. k-correction estimated by different authors. The solid line corresponds to the median value, dashed line show the one to one relation and error bars correspond to the 10 and 90 percentiles associated to the median. The large scatter between different methods can be appreciated.

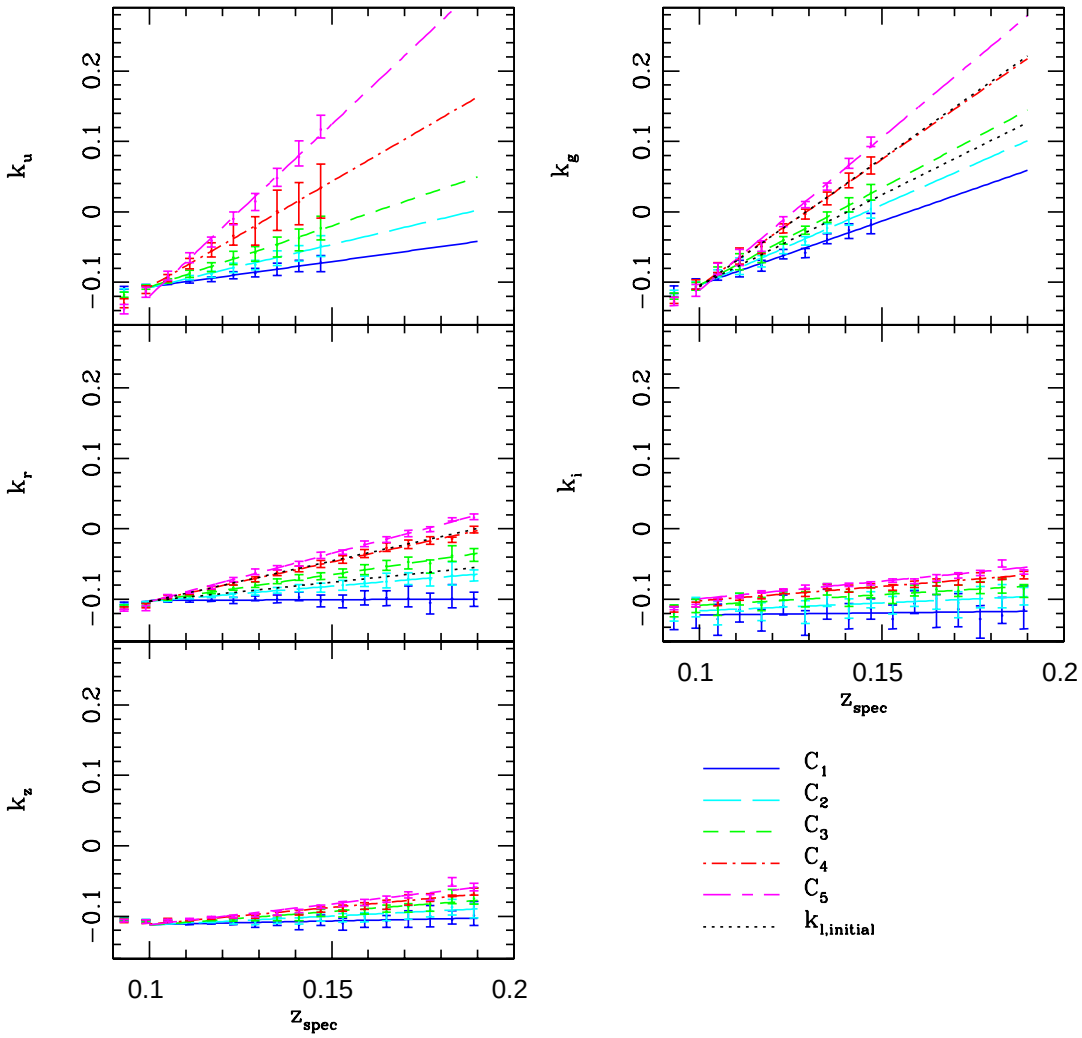

Figure 4. Median K-correction estimates for the 5 SDSS photometric bands u, g, r, i and z. The lines represent the fit to the median for 5 cuts in reference-colour index $(g-r)$. The error bars corresponds 25 and 75 percentiles from the median. The dotted lines in k_g and k_r represent the initial k values for the iteration (see text).

age PSF. For SDSS, a galaxy with $M_r = -23$ has a z_{max} of 0.63 (see O'Mill et al. (2008) Table 1). For this reason, we recommend using galaxies with $z_{\rm phot} \leqslant 0.6$.

4 K CORRECTIONS

k-corrections allow to transform the observed magnitudes at a redshift z, into standard luminosities at some reference frame. This correction depends on the filter that was used for the observations, the rest-frame standard, the shape of the SED of the galaxy, and the redshift (see Hogg et al. (2001)).

In the previous sections we have used Artificial Neural Network as a tool to perform non-linear fitting to obtain photometric redshifts. An analysis based on a neural network approximation is the natural trend to obtain k-corrections. However these techniques needs a large and representative amount of prior information in the form of a training set.

The problem with the former is the lack of confidence on individual k-corrections estimates. This is shown in Figure 3 where we compare r-band k-corrections estimated by different authors for 6113 galaxies, selected randomly from MGS, in the narrow redshift range 0.14<z<0.16. For Blanton & Roweis (2007) we use `k-correct_v4.2`, for Chilingarian et al. (2010) we employed the on-line available code [4], for Westra et al. (2010) we used the on-line empirical k-correction calculator [5] and using models and (g-r) parameter and we also compare with k-corrections downloaded from the SDSS `Photoz` table (Abazajian et al. (2009)).

It is clear that individual estimates have a large uncertainty as indicated by the large scatter between different methods, whereas the mean trends can be trusted.

[4] http://kcor.sai.msu.ru/getthecode/
[5] http://tdc-www.cfa.harvard.edu/instruments/hectospec/progs/EOK/

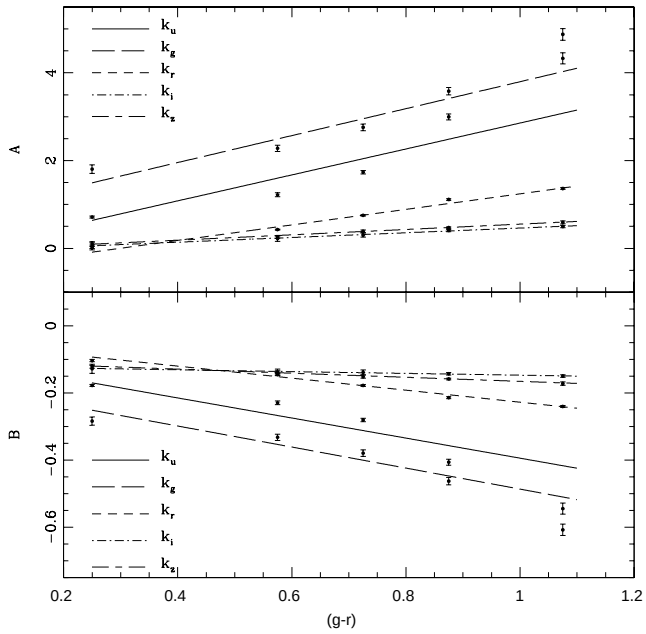

Figure 5. A and B coefficients for the K correction fits of the form $k = Az + B$ where $A = a_A(g-r) + b_A$ and $B = a_B(g-r) + b_B$

Since the development of the public code k-correct[6] (Blanton et al. (2003)) many authors have used this method to calculate k-corrections. This code is based on a mathematical algorithm, namely a non-negative matrix factorization, which creates model based template sets. The set of templates is reduced to a basis of the five SDSS pass bands, which are used to interpret the SED of the galaxy in terms of stellar populations. Then, linear combinations of these templates are used to fit spectral energy distributions to broadband photometric observations for each galaxy and so k-corrections are obtained.

The disadvantage of this method is the use of a limited number of spectra that decreases with distance. The intrinsic colour of a galaxy is related to its SED, therefore this property can be used to compute k-corrections at high redshifts, where the Blanton's k-correction technique is more uncertain.

In this paper we use the public available code described in Blanton & Roweis (2007) (`k-correct_v4.2`) as a tool for calibrate our k-corrections.

4.1 Model for k-corrections

The use of galaxy colours to describe galaxy populations presents the advantage that colours are easily quantifiable rather than morphological types. In this work we analyse a relation between k-corrections and the reference-frame galaxy $(g-r)$ colour index.

As described in Section 2, Sk1 sample comprises MGS up to $z \sim 0.2$. Since the motivation of this work is to derive k-corrections at higher redshifts, we have calculated k-corrections for the Sk1 sample using the `k-correct_v4.2` code, analysed their dependence on the galaxy reference frame $(g-r)$ colour and extrapolate the results obtained to higher redshifts. Following Blanton & Roweis (2007), k-corrections were calculated on the five SDSS photometric bands shifted to $z_{spec} = 0.1$.

We divide the spectroscopic data into five different sub-samples (C_i) according to the reference-frame $(g-r)$ colour:

C_1: $(g-r) < 0.5$,
C_2: $0.5 < (g-r) < 0.65$,
C_3: $0.65 < (g-r) < 0.8$,
C_4: $0.8 < (g-r) < 0.95$,
C_5: $(g-r) > 0.95$.

Then we calculate median values of k-corrections per redshift interval for the different C_i sub-samples, for the five SDSS bands. The results are shown in Figure 4 where it can be appreciated the smooth dependence of the median k-correction values as a function of redshift once the reference galaxy $(g-r)$ colour is taken into account. We consider galaxies with $z \geqslant 0.1$ and we adopt a linear relation $k = Az + B$ for each C_i sub-sample. The resulting fits are also displayed in Figure 5 where the error bars correspond to 25 and 75 percentiles of the median values.

By inspection of this figure it can be seen that our linear model is a good representation of the relation between k-correction and redshift.

The values of the parameters A and B are obtained by fitting a straight line through χ^2 minimization for each C_i sub-sample. In Figure 5 we plot the derived values of A (upper panel) and B (bottom panel) as a function of the mean $(g-r)$ values for each C_i sub-sample; the error bars correspond to the square root of the variances in the estimates of A and B from χ^2 minimization. From this figure it can been seen that a linear relation also gives a fair representation of the trends observed. Therefore, we adopt a model where $A = a_A(g-r) + b_A$ and $B = a_B(g-r) + b_B$. The final calibration of Blanton's k-corrections is given as

$$k_j = [a_{Aj}(g-r) + b_{Aj}]z + [a_{Bj}(g-r) + b_{Bj}] \qquad (1)$$

where j represents the different $ugriz$ bands.

[6] http://howdy.physics.nyu.edu/index.php/Kcorrect

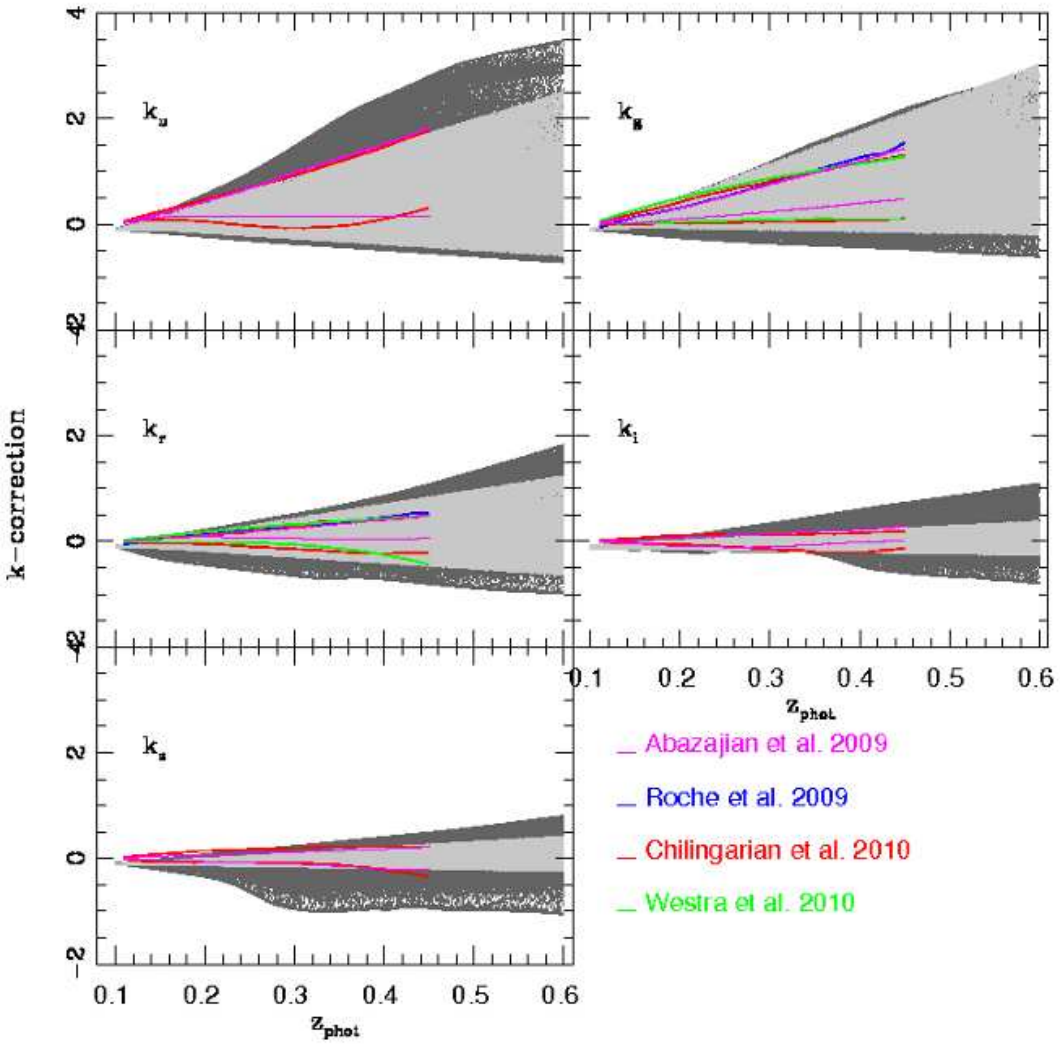

Figure 6. k-correction obtained for a random sample of SDSS-DR7 galaxies. Our estimates are shown in grey and in dark-grey we provide the results using Blantons 2003 code. Blue solid lines are k-corrections obtained for early-type galaxies presented in Roche et al. (2009), red solid lines k-correction computed using "K-correction calculator" (Chilingarian et al. (2010)), magenta solid lines corresponds to Abazajian et al. (2009) estimates and in green solid lines Westra et al. (2010) k-corrections.

In Table 2 we present the a_{Aj}, b_{Aj}, a_{Bj} and b_{Bj} values and the errors obtained by χ^2 minimization.

4.2 Estimation of k-corrections

In order to compute k-corrections using the model described in the previous Section, it is necessary to obtain reference-frames $(g-r)$ colours for each galaxy, which in turn depends on k-corrections.

To avoid this problem we have adopted an iterative procedure as follows: the iteration starts with an initial value for k_g and k_r according to the value of the concentration index of the galaxy in the r band (c_r). This quantity does not depend on k-correction and is a suitable indicator of galaxy morphological type bimodality: early-type galaxies have higher c_r than later types (Strateva et al. (2001), Kauffmann et al. (2003a), Kauffmann et al. (2003a), Mateus et al. (2006)).

According to Strateva et al. (2001), $c_r > 2.55$ values correspond to early-type galaxies, and late-type galaxies have $c_r < 2.55$. This bimodality can also be seen in the colour distribution of galaxies. In particular, the distribution of $(g-r)$ colours has two well-defined peaks: one at $(g-r) = 0.60$ and other at $(g-r) = 0.95$, corresponding to the late and early-type components, respectively. Taken these properties into account, we assign $(g-r)_{initial} = 0.60$ if $c_r < 2.55$ and $(g-r)_{initial} = 0.95$ if $c_r > 2.55$ so that the initial k_g and k_r values are:

$$k_{l,initial} = [a_{Al}(g-r)_{initial} + b_{Al}]z + [a_{Bl}(g-r)_{initial} + b_{Bl}],$$

where l refers to the g and r bands (see the dotted lines Figure 4)

Once these initial values are fixed, we iterate in equation 1 to obtain k_g and k_r for each galaxy. After each iteration, we check that the colours are within an acceptable range, $0 < (g-r) < 1.8$ in order to avoid either too red or too blue colours. In these cases the iteration starts again with a new $(g-r)_{initial}$ value selected at

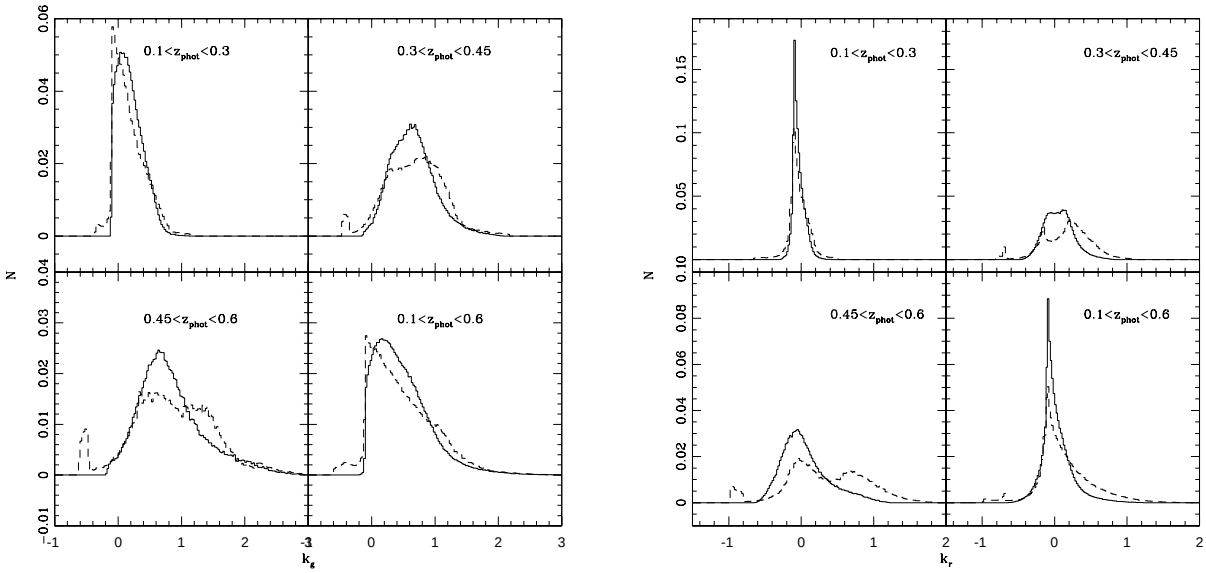

Figure 7. k_g and k_r obtained for Sk2 sample in a 4 different redshift cuts. Our estimates are shown in solid lines and in dashed histogram we provide the results using `k-correct_v4.2`

Table 2. Parameters of the $k_j = [a_{Aj}(g-r) + b_{Aj}]z + [a_{Bj}(g-r) + b_{Bj}]$ relation obtained by χ^2 minimization

Band	a_A	σ_{a_A}	b_A	σ_{b_A}	a_B	σ_{a_B}	b_B	σ_{b_B}
u	2.956	0.070	−0.100	0.034	−0.299	0.009	−0.095	0.004
g	3.070	0.165	0.727	0.117	−0.313	0.021	−0.173	0.015
r	1.771	0.032	−0.529	0.023	−0.179	0.005	−0.048	0.003
i	0.538	0.085	−0.075	0.079	−0.027	0.013	−0.120	0.012
z	0.610	0.045	−0.064	0.034	−0.061	0.007	−0.106	0.005

random from a Gaussian distribution (within 1σ) that fits either the blue or the red peak of the reference frame colour distribution.

The iterations stop when the difference in both k_g and k_r between two consecutive steps is less than 0.001. This procedure converges in less than 15 iterations.

From the finally obtained k_g and k_r values we calculate the reference frame $(g-r)$ colours, which allows to compute k-corrections in the other bands using equation 1.

We notice that there is a small percentage (less than 0.4%) of galaxies for which our algorithm does not converge. However, the main sources for this lack of convergence are large magnitude uncertainties and unreliable observed colours($(g-r)_{obs} > 3$). The last colours constraints are helpful on removing stars with unusual colours, without discarding real galaxies (Lopes (2007), Padmanabhan et al. (2005)). Collister et al. (2007) point out that the stellar contamination may still be present.

4.3 Results

We have compared the k-corrections obtained in this work with the results from `k-correct_v4.2` using the Sk2 sample. As explained in Section 2, we have restricted our analysis to galaxies with $r < 21.5$.

In Figure 6 we plot both estimations against redshift for the five SDSS-DR7 bands. In dark-grey we show `k-correct_v4.2` results whereas light-grey points are our estimates. It can bee seen in all cases, that our k-correction shows the same trend but with a lower spread than Blanton & Roweis (2007) results. This lower spread is particularly noticeable in the i and z bands. However, our estimations are in agreement with Chilingarian et al. (2010) k-corrections in these bands. In Figure 6 we also compare our k-corrections with those obtained for $E/S0$ galaxies by Roche et al. (2009). We find that the mean k-correction for the early type galaxies lies within our estimates for red galaxies (C_5 sample), where k-correction values are higher. We also perform a comparison with k-corrections obtained using the "K-correction calculator" (Chilingarian et al. (2010)), the "on-line empirical k-correction calculator" (Westra et al. 2010) and k-corrections from `Photoz` table (Abazajian et al. 2009). We compute the k-corrections in all bands at extreme red and blue colours, finding that these estimates are within our range of calibrated values. We notice a difference in the k_u for blue galaxies at higher redshift with respect to Chilingarian et al. (2010). We argue that this can be originated in the fact that these authors calibrate k_u with the $u-r$ colour and that the u filter has a natural red leak that cases abnormal $u-r$ colours. This effect can propagate to the k-corrections, generating higher values, particularly at large redshifts.

In Figure 7 we plot the distributions of k_g and k_r in four dif-

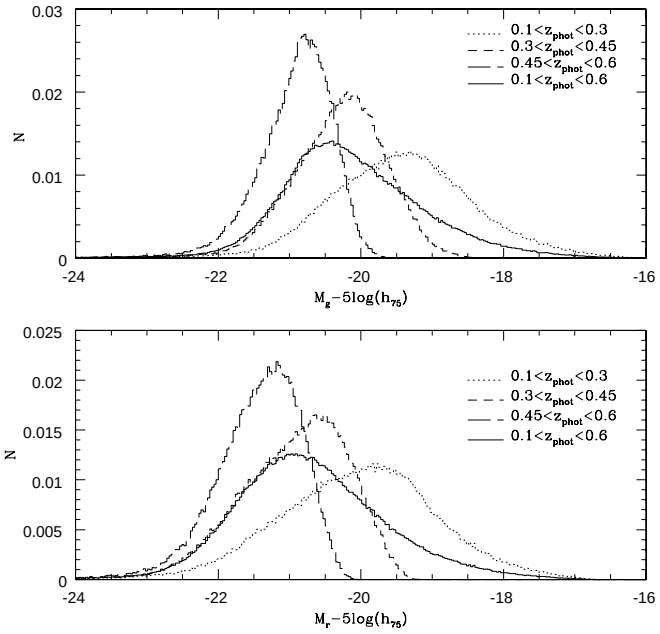

Figure 8. Luminosity distribution for galaxies brighter than $M_r - 5log(h_{75}) = -21.5$ and for 4 different redshifts cuts.

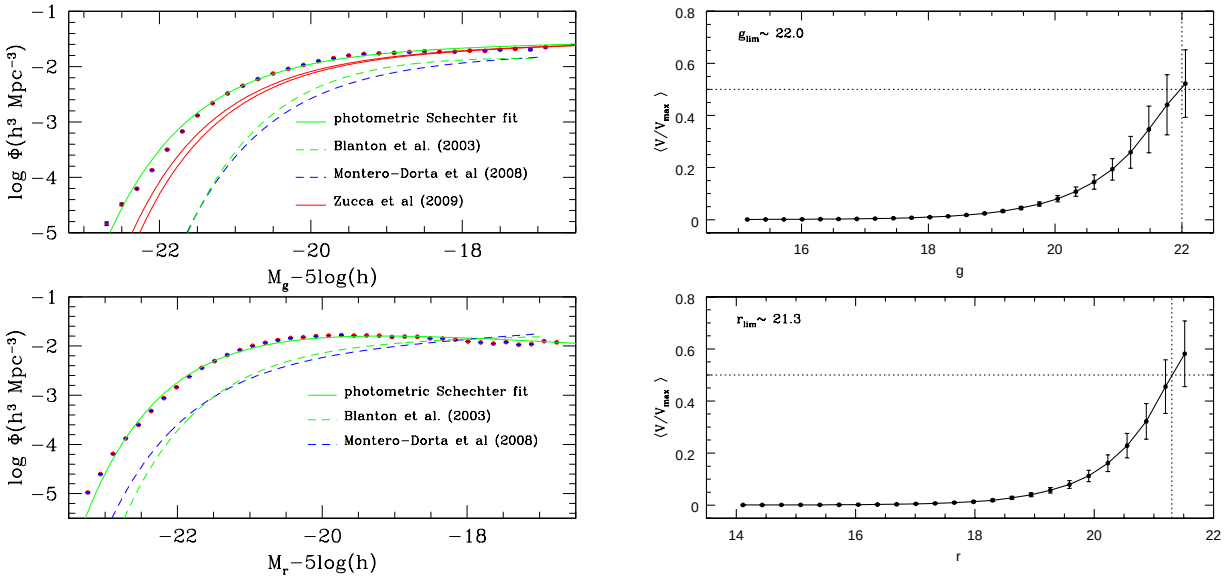

Figure 9. Left panel: Luminosity function in g and r bands. The dashed lines show the Schecter fit for MGS of Blanton et al. (2003) and Montero-Dorta & Prada (2009) (green and blue respectively). The green solid line is the result from the $1/Vmax$ method for our photometric sample. The red solid lines are the result from the STY method from two different redshift bins ($0.1 < z < 0.35$ and $0.35 < z < 0.55$) from Zucca et al. (2009). The error bars (blue colours) represent 1σ uncertainty calculated using a bootstrapping technique. Right panels: $V/Vmax$ test. The error bars represent 1σ deviation from the median. The horizontal dotted lines at $V/Vmax = 0.5$ correspond to the g and r band completeness.

ferent redshift intervals. Our estimates are shown as solid lines, and the dashed histogram is `k-correct_v4.2` code (Blanton & Roweis 2007) results. For galaxies in the redshift range $0.1 < z_{\rm phot} < 0.3$, both distributions are similar. As redshift increases, our distributions remain always unimodal, with a well defined mean. On the other hand, Blanton's k-correction distribution shows 3 different maxima, one centered approximately in our distribution, and the others in the extremes. This behavior is probably indicative of template mismatch. At redshifts $0.1 < z_{\rm phot} < 0.6$, both k_r distributions approximately match each other, whereas g-band k-corrections from `k-correct_v4.2` distribution is lopsided to negative values.

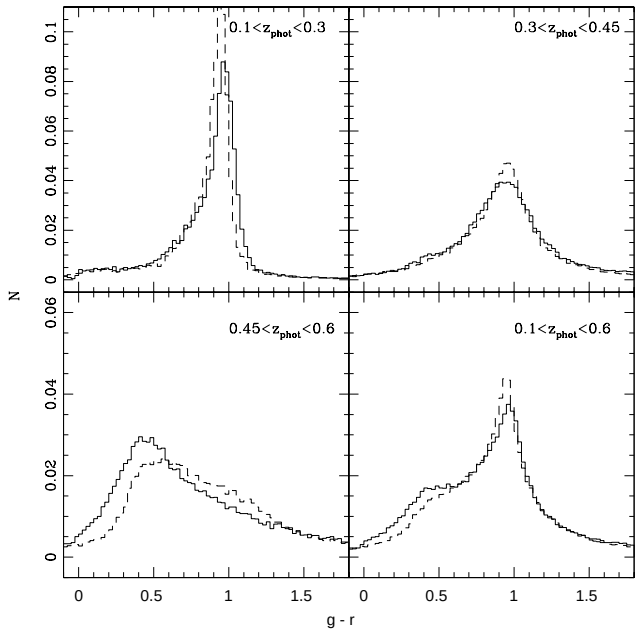

Figure 10. Derived rest frame $(g-r)$ colour distribution for galaxies brighter than $M_r - 5log(h_{75}) = -21.5$ and for 4 different redshifts cuts in Sk2 sample. The dashed histogram corresponds to Blanton's 2003 results and in solid lines our estimates. Relative excess of red galaxies in Blantons results is clearly seen in comparison to our colour estimates

4.4 Luminosities and colours

We have estimated the absolute magnitude of galaxies in the Sk2 sample in the g and r bands using our k-corrections. The absolute magnitude of a galaxy in a given band is related to its apparent magnitude by:

$$M_l = l - 5log_{10}(DL(z)) - 25 - k_l$$

where l refers to the g and r bands, and $DL(z)$ is the luminosity distance (which depends on the cosmological parameters adopted). In Figure 8, we show the distribution of k-corrected absolute magnitudes in four different increasing redshift intervals (key in Figure). The shape of these distributions is very similar in both g and r SDSS bands: a bell-shaped distribution skewed to fainter magnitudes. Notice that the mean of the distributions move towards fainter magnitudes as the redshift range decreases, while the bright tail of the distribution remains approximately fixed at $M_g \sim -22.5$ and $M_r \sim -23$.

For Sk2 photometric sample we computed the luminosity function in the g and r bands using the $1/Vmax$ method considering the incompleteness with a $V/Vmax$ test (Schmidt (1968)). This methods takes into account the volume of the survey enclosed by the galaxy redshift and the difference between the maximum and minimum volumes within which it can be observed.

In Figure 9 we show the luminosity function and $V/Vmax$ test for the redshift range $0.1 < z_{\rm phot} < 0.6$. The dashed lines show the Schechter fit for MGS of Blanton et al. (2003) and Montero-Dorta & Prada (2009). The green solid line is the resulting Schechter fit for Sk2 sample. We compared our result in g band ($4686\mathring{A}$) with two different redshift bins from Zucca et al. (2009). These authors have studied the evolution in the B band ($4459.7\mathring{A}$) luminosity function to redshift $z \sim 1$ in the $zCOSMOS$ from the STY method.

Our best Schechter fit corresponds to $M^\star \sim -20.469 \pm 0.0535$, $\Phi^\star \sim 0.0224 \pm 0.0089$ and $\alpha \sim -1.065 \pm 0.0286$ for g band, and $M^\star \sim -20.821 \pm 0.0966$, $\Phi^\star \sim 0.030 \pm 0.0029$ and $\alpha \sim -0.78 \pm 0.0298$ for r band. Where the errors had been obtained through bootstrapping. We notice that the luminosity functions at $z \sim 0.5$ from our work and that of Zucca et al. (2009) are consistent taking into account the $(g-B)$ values of typical Sbc galaxies at this redshift (Fukugita et al. 1995).

In Figure 10 we compare the $(g-r)$ colour distribution of galaxies brighter than $M_r = -21.5$ in four redshift intervals. The dashed histogram corresponds to `k-correct_v4.2` code results, and in solid lines we show our estimates. For galaxies with $0.1 < z_{\rm phot} < 0.3$ both distributions are similar, exhibiting a prominent red peak corresponding to early-type galaxies. As redshift increases, the distributions are shifted bluewards, and we notice in the redshift range $0.45 < z_{\rm phot} < 0.6$ an excess of red galaxies in Blanton & Roweis (2007) results in comparison to ours. This trend can also be seen in the full redshift range (Figure 10 bottom right panel), where the galaxy bimodality can also be appreciated.

In Figures 11 and 12 we show the colour-colour diagrams $(g-r)$ vs $(r-i)$ and $(g-r)$ vs $(i-z)$ for galaxies brighter than $M_r = -21.5$ in four different redshift intervals. The contours enclose 50%, 65% 85%, and 90% of the galaxies in Sk2 sample. In all cases the shaded region represents the corresponding colour-colour diagram for 90% of MGS, which have spectroscopic redshifts. The left upper panel ($0.1 < z_{\rm phot} < 0.2$) shows that contours calculated for the photometric sample matches the shaded region. As the redshift increases, the contours in the colour-colour diagrams expand with respect to the spectroscopic sample, but both have approximately the same center. The expansion of the contours for the photometric results could be due to uncertainties in the determination of photometric redshifts and k-corrections, as well as they may reflect galaxy evolution. The colours show a decreasing trend

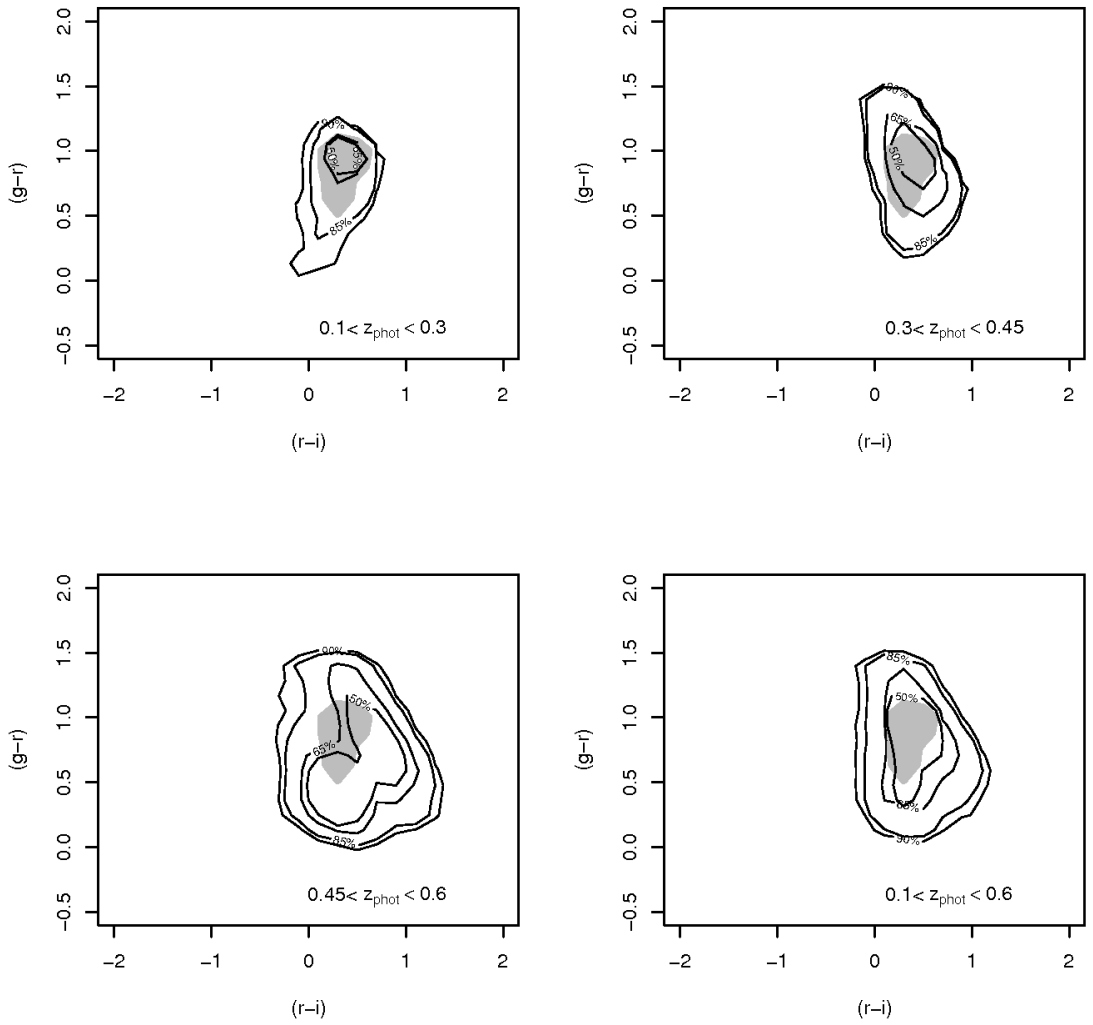

Figure 11. $(g-r)$ vs $(r-i)$. colour-colour diagram for galaxies brighter than $M_r = -21.5$ in four different redshift intervals for Sk2 sample. The contours enclose 50%, 65% 85%, and 90% of the photometric sample. The shaded region represents the colour-colour diagram for 90% of MGS.

for the red population as well as a constant shift to bluer colours (O'Mill et al. (2008)). This is particularly important for the redshift range $0.45 < z_{\rm phot} < 0.6$.

5 CONCLUSIONS

In this work we present a new set of photometric redshift ($z_{\rm phot}$) and k-correction estimations for the SDSS-DR7 photometric catalogue available on the World Wide Web. In order to calculate $z_{\rm phot}$, artificial neural networks were applied using the public code ANNz. The improvements in the SDSS-DR7 photometric redshift estimation are:
1) We added the concentration index and the Petrossian radii in g and r bands to the usual five magnitudes used in previous similar works. These additional inputs improve $z_{\rm phot}$ estimations because the concentration index provides information regarding the slope of the galaxy brightness profile, helping us to break the degeneracies in the redshift-colour relation due to morphology. The Petrossian radius is a robust measure of how shallow the brightness profile is and contain information about the angular size, that is related to the distance.
2) The choice of different galaxy samples for the training set (MGS, LRG and AGN sample) provides a wide sampling of different galaxy types at various redshifts, allowing to improve $z_{\rm phot}$ estimates.

Our $z_{\rm phot}$ estimates have a $rms \simeq 0.0227$, and the resulting galaxy distribution shows a good agreement with the theoretical distribution derived from the SDSS galaxy luminosity functions.

We have used the `k-correct_v4.2` code (Blanton & Roweis (2007)) for the MGS and we have performed a linear fit between reference frame $(g-r)$ colour and redshift, extrapolating this relation at high redshifts. We propose an iterative procedure to estimate k-corrections from the observed photometry in the g and r bands. Using initial values that depend on the concentration index and the observed colour, we obtain the k-correction for the other bands. Our results show that the use of this simple linear re-

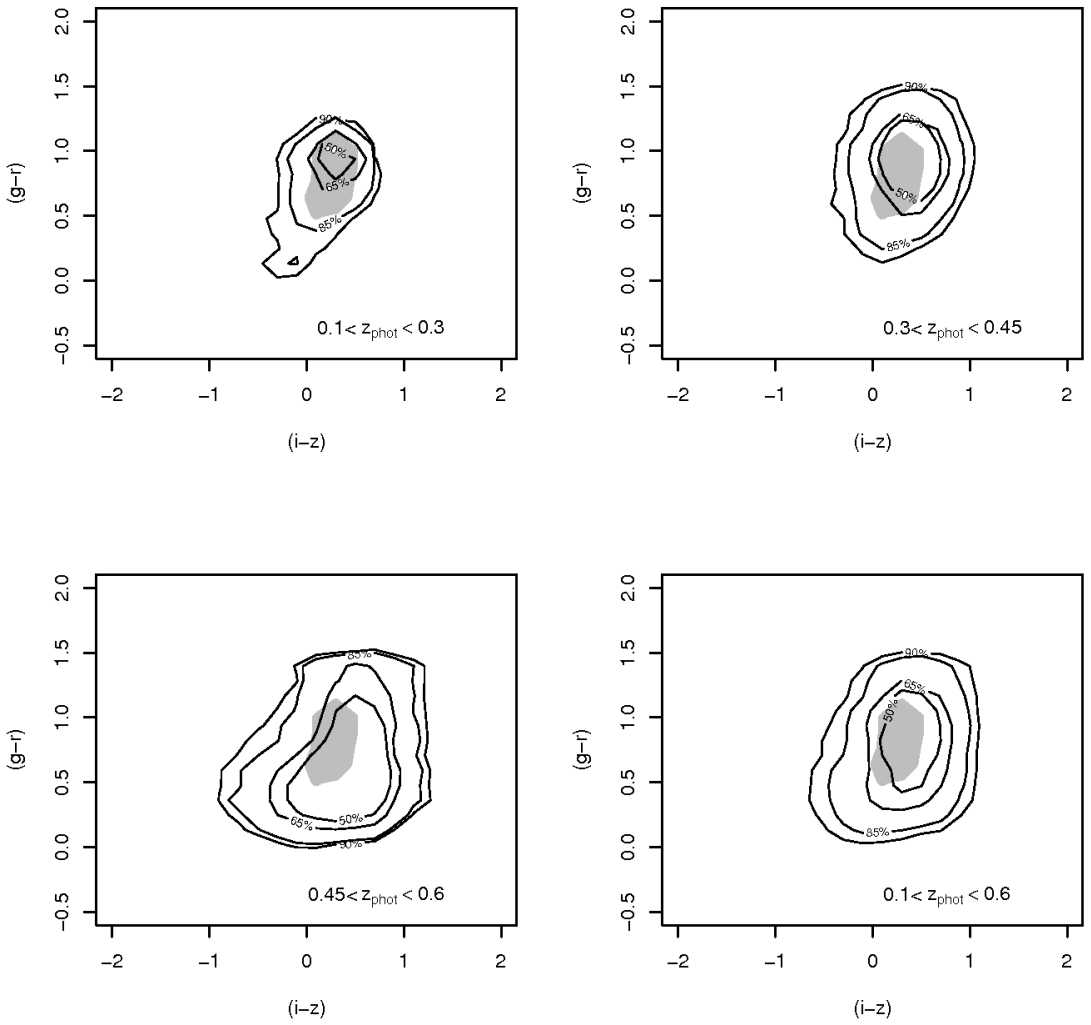

Figure 12. $(g-r)$ vs $(i-z)$ colour-colour diagram for galaxies brighter than $M_r = -21.5$ in four different redshift intervals for Sk2 sample. The contours enclose 50%, 65% 85%, and 90% of the photometric sample. The shaded region represents the colour-colour diagram for 90% of MGS.

lation between the reference frame $(g-r)$ colour and redshift is as accurate as those obtained in previous work. A clear plus of our approach is the low computational time.

Our k-correction estimations do not use templates, avoiding statistical errors in the lack of homogeneity in spectral features, and minimizing systematical errors caused by an assumed spectral energy distribution (SED). This can be noticed in the smooth behavior of the distribution of k-corrections, even for intermediate redshifts.

The analysis of the distribution of k-corrected absolute magnitudes show that the shape of these distributions has a bell-shaped skewed to fainter magnitudes and the mean of the distributions move towards fainter magnitudes as the redshift range decreases.

We have computed the luminosity function in g and r bands trhough $1/Vmax$ method taking into account the incompleteness with a $V/Vmax$ test (Schmidt (1968)). We notice that the curves derived from this work and that of Zucca et al. (2009) are consistent taking into account the $(g-B)$ value of a typical Sbc galaxy at $z \sim 0.5$ Fukugita et al. (1995).

The analysis of the $(g-r)$ colour distribution for galaxies brighter than $M_r = -21.5$ shows that the galaxies in our samples are shifted bluewards as redshift increases. This trend leads to the emergence of bimodality in the full redshift range. From the colour-colour diagrams, we can conclude that the behavior of colours at low redshift is in good agreement with the trends of the spectroscopic sample. As redshift increases we see a broadening of the contours and an increase in the blue galaxy population. However, the distribution of galaxies in the colour-colour diagram remains centered with respect to the spectroscopic data.

6 ACKNOWLEDGMENTS

We thank the Referee for very helpful comments which that greatly improved this paper. We thank William Schoenell and the The SEAGal/STARLIGHT Project. This work was supported in part by the Consejo Nacional de Investigaciones Científicas y Técnicas de la República Argentina (CONICET), Secretaría de Ciencia y Tec-

nología de la Universidad dad de Córdoba. Laerte Sodré Jr was supported by the Brazilian agencies FAPESP and CNPq. Funding for the SDSS and SDSS-II has been provided by the Alfred P. Sloan Foundation, the Participating Institutions, the National Science Foundation, the U.S. Department of Energy, the National Aeronautics and Space Administration, the Japanese Monbukagakusho, the Max Planck Society, and the Higher Education Funding Council for England. The SDSS Web Site is http://www.sdss.org/. The SDSS is managed by the Astrophysical Research Consortium for the Participating Institutions. The Participating Institutions are the American Museum of Natural History, Astrophysical Institute Potsdam, University of Basel, University of Cambridge, Case Western Reserve University, University of Chicago, Drexel University, Fermilab, the Institute for Advanced Study, the Japan Participation Group, Johns Hopkins University, the Joint Institute for Nuclear Astrophysics, the Kavli Institute for Particle Astrophysics and Cosmology, the Korean Scientist Group, the Chinese Academy of Sciences (LAMOST), Los Alamos National Laboratory, the Max-Planck-Institute for Astronomy (MPIA), the Max-Planck-Institute for Astrophysics (MPA), New Mexico State University, Ohio State University, University of Pittsburgh, University of Portsmouth, Princeton University, the United States Naval Observatory, and the University of Washington.

REFERENCES

Abazajian, K. N., et al. 2009, ApJS, 182, 543
Abdalla, F. B., Banerji, M., Lahav, O., & Rashkov, V. 2008, arXiv:0812.3831
Banerji, M., et al. 2010, MNRAS, 406, 342
Benitez, N. 2000, ApJ, 536, 571
Benitez, N. 1998, Abstracts of the 19th Texas Symposium on Relativistic Astrophysics and Cosmology, held in Paris, France, Dec. 14-18, 1998. Eds.: J. Paul, T. Montmerle, and E. Aubourg (CEA Saclay), meeting abstract.
Bishop, C. M., 1991 "A fast procedure for retraining the multilayer perceptron", International Journal of Neural Systems 2(3), 229236
Blanton, M. R., et al. 2003, AJ, 125, 2348
Blanton, M., & Roweis, S. 2007, AJ, 133, 734.
Bolzonella, M., Miralles, J.-M., & Pelló, R. 2000, A&A, 363, 476
Brunner, R. J., Djorgovski, S. G., Gal, R. R., & Odewahn, S. C. 1999, Bulletin of the American Astronomical Society, 31, 1492
Budavári, T., et al. 2001, AJ, 122, 1163
Chilingarian, I. V., Melchior, A.-L., & Zolotukhin, I. Y. 2010, MNRAS, 405, 1409
Collister, A., et al. 2007, MNRAS, 375, 68
Collister, A. A., & Lahav, O. 2004, PASP, 116, 345
Connolly, A. J., Csabai, I., Szalay, A. S., Koo, D. C., Kron, R. G., & Munn, J. A. 1995, AJ, 110, 2655
Csabai, I., et al. 2003, AJ, 125, 580
Eisenstein, D. J., et al. 2001, AJ, 122, 2267
Fukugita, M., Ichikawa, T., Gunn, J. E., Doi, M., Shimasaku, K., & Schneider, D. P. 1996, AJ, 111, 1748
Fukugita, M., Shimasaku, K., & Ichikawa, T. 1995, PASP, 107, 945
Gunn, J. E., et al. 1998, AJ, 116, 3040
Hogg, D. W., Baldry, I. K., Blanton, M. R., & Eisenstein, D. J. 2002, arXiv:astro-ph/0210394
Hogg, D. W., Blanton, M., & SDSS Collaboration 2001, Bulletin of the American Astronomical Society, 34, 570
Humason, M. L., Mayall, N. U., & Sandage, A. R. 1956, AJ, 61, 97
Kauffmann, G., et al. 2003a, MNRAS, 341, 33
Kauffmann, G., et al. 2003, MNRAS, 346, 1055
Lahav, O., et al. 1995, Science, 267, 859
Lopes, P. A. A. 2007, MNRAS, 380, 1608
Mannucci, F., Basile, F., Poggianti, B. M., Cimatti, A., Daddi, E., Pozzetti, L., & Vanzi, L. 2001, MNRAS, 326, 745
Mateus, A., Sodré, L., Cid Fernandes, R., Stasińska, G., Schoenell, W., & Gomes, J. M. 2006, MNRAS, 370, 721
Montero-Dorta, A. D., & Prada, F. 2009, MNRAS, 399, 1106
Oke, J. B. & Sandage, A. 1968, ApJ, 154, 21
O'Mill, A. L., Padilla, N., & García Lambas, D. 2008, MNRAS, 389, 1763
Oyaizu, H., Lima, M., Cunha, C. E., Lin, H., Frieman, J., & Sheldon, E. S. 2008, ApJ, 674, 768
Padmanabhan, N., et al. 2005, MNRAS, 359, 237
Pier, J. R., Munn, J. A., Hindsley, R. B., Hennessy, G. S., Kent, S. M., Lupton, R. H., & Ivezić, Ž. 2003, AJ, 125, 1559
Roche, N., Bernardi, M., & Hyde, J. 2009, MNRAS, 398, 1549
Schmidt, M. 1968, ApJ, 151, 393
Shapley, H. 1932, Annals of Harvard Observatory, Cambridge: Harvard Observatory, 1932
Smith, J. A., Tucker, D. L., Allam, S. S., & Jorgensen, A. M. 2002, Bulletin of the American Astronomical Society, 34, 1272
Strauss, M. A., et al. 2002, AJ, 124, 1810
Strateva, I., et al. 2001, AJ, 122, 1861
Westra, E., et al. 2010, 2010arXiv1006.2823W
York, D. G., et al. 2000, AJ, 120, 1579
Zucca, E., et al. 2009, A&A, 508, 1217